Available online at www.sciencedirect.com
ScienceDirect
Trans. Nonferrous Met. Soc. China 29(2019) 2109−2116
Transactions of Nonferrous Metals Society of China
www.tnmsc.cn

Effect of Al and Sc on deformation behavior of FeCoNi multi-element alloys

Rui ZHOU[1], Mou LI[1], Jing-wen QIU[1,2], Si-hui OUYANG[1], Di PAN[1], Cheng-shang ZHOU[1], Yong LIU[1]

1. State Key Laboratory of Powder Metallurgy, Central South University, Changsha 410083, China;
2. Hunan Provincial Key Laboratory of High Efficiency and Precision Machining of Difficult-to-Cut Material, Hunan University of Science and Technology, Xiangtan 411201, China

Received 30 May 2019; accepted 27 September 2019

Abstract: The effects of Al and Sc on mechanical properties of FeCoNi multi-element alloys (MEAs) were investigated by compressive tests. The microstructures of FeCoNi MEAs with different contents of Al and Sc were characterized and the strengthening mechanisms were discussed. The results show that FeCoNi MEA with a low content of Al has a face-centered cubic (FCC) structure. The yield strength increases linearly with the increase of Al content, which is largely caused by solid solution hardening. Further addition of Sc can promote the formation of a new phase in $(FeCoNi)_{1-x}Al_x$ MEAs. A minor addition of Sc can significantly increase the yield strengths of $(FeCoNi)_{1-x}Al_x$ MEAs with a low Al content and improve the compressive plasticity of $(FeCoNi)_{1-x}Al_x$ MEAs with a high Al content.

Key words: FeCoNi multi-element alloys; mechanical properties; microstructure; strengthening mechanism

1 Introduction

Multi-element alloys (MEAs) containing several major alloying elements with equimolar or near-equimolar compositions have a good combination of mechanical properties [1]. Although with multi elements, the alloys still have simple solid solution structures, such as face-centered cubic (FCC) or body-centered cubic (BCC) [2,3]. Previous studies show that MEAs have high hardness, high oxidation resistance, high wear resistance and good corrosion properties [4−8]. Moreover, ternary MEAs mostly exhibit higher mechanical properties than the quaternary and quinary MEAs [9]. As a typical ternary MEA, FeCoNi alloy has been widely investigated and exhibits excellent ductility but insufficient yield strengths [10].

It is well known that the addition of Al is an effective approach to improve the yield strength of FeCoNiCr-based MEAs. It has been revealed that an increase of hardness in $Al_xFeCoCrNi$ was induced by the increase of Al content [11]. When the Al content increased from 0.25 to 1 at.%, the yield strength of $Al_xCoFeNi$ MEAs raised from 158 to 967 MPa [12]. The small amount of Al addition also caused the increase of the hardness for $Al_xCoCrCuFeNi$ MEAs [13]. These improvements of mechanical properties in FeCoNiCr-based MEAs are mainly due to the severe lattice distortion effect and solid solution strengthening from the addition of Al.

Moreover, the addition of Al can promote forming intermetallic compound that may serve as dispersed strengthening precipitates in MEAs to enhance the mechanical properties. HE et al [14] found that the tensile strength of $(FeCoNiCr)_{94}Ti_2Al_4$ MEAs was improved significantly with the help of $L1_2$ nano-precipitates. YANG et al [15] indicated that a small addition of Al and Ti in FeCoNi-based MEAs can bring the uniform distribution of multi-component intermetallic nano-particles and enhance the tensile strength without sacrificing the ductility.

Scandium (Sc) is also a promising element to form compounds with good thermal stability [16]. A minor Sc addition in Al matrix can achieve coherent strengthening precipitates of Al_3Sc which improved mechanical properties of Al−Mg−Sc alloys by precipitation strengthening [17]. TAENDL et al [18] found that the Al_3Sc precipitates in Al−Mg−Sc−Zr alloys are fine and

Foundation item: Projects (51671217, 51604112) supported by the National Natural Science Foundation of China; Project (2017JJ3089) supported by the Natural Science Foundation of Hunan Province, China
Corresponding author: Jing-wen QIU; E-mail: qjwcsu@foxmail.com
DOI: 10.1016/S1003-6326(19)65117-4

homogeneous, which help to refine grains. Thus, Al and Sc elements can be considered as promising candidates to strengthen MEAs. However, the study on the Al and Sc-containing MEAs is still rare.

In this work, Al element was added in FeCoNi MEAs to introduce significant solid solution hardening. And a minor amount of Sc was added in $(FeCoNi)_{1-x}Al_x$ MEAs in order to form strengthening precipitates. After arc-melting, $(FeCoNi)_{1-x}Al_x$ and Sc-containing $(FeCoNi)_{1-x}Al_x$ MEAs were obtained, and the compressive properties were tested. The microstructures were characterized to clarify the strengthening mechanisms.

2 Experimental

$(FeCoNi)_{1-x}Al_x$ (x=5−9, 23 at.%) and Sc-containing $(FeCoNi)_{1-x}Al_x$ MEAs were fabricated by arc-melting in argon. The addition of Sc is 0.01, 0.1, 0.3 and 0.5 at.%, respectively. The purity of raw elements was above 99.9 wt.%. The ingots were flipped and re-melted over five times to achieve homogeneous mixing. An X-ray diffractometer (XRD, Rigaku D/MAX−2250) with Cu K_α radiation was used to identify the phases of MEAs. The microstructures and chemical composition of MEAs were characterized by a scanning electron microscope (SEM) (FEI Nova Nano230) with an energy dispersive X-ray (EDX) analyzer. The standardized (GB T7314−1987) ingots with a diameter of 6 mm were shaped by wire-electrode cutting. Compressive tests were performed on an Instron 3369 machine at room temperature with an engineering strain rate of 5×10^{-3} s^{-1}.

3 Results

Figure 1(a) shows the XRD patterns of the as-cast $(FeCoNi)_{1-x}Al_x$ MEAs. It can be seen that the lowest Al content (x=5 at.%) MEA has a single FCC crystal structure. As higher contents of Al (x=6−9 at.%) were added, the MEAs maintain FCC crystal structure. When x reached 23 at.%, only BCC phase was detected. $(FeCoNi)_{1-x}Al_x$ MEAs (x=6−9 at.%) clearly indicate the presence of three different major peaks at different 2θ of around 45°, 50° and 70°. The $(FeCoNi)_{1-x}Al_x$ MEA with 5 at.% Al exhibits only one peak (at 2θ of around 50°), which is different from patterns of the FCC structure in the specimens (x=6−9 at.%). This may be caused by the small number of grains in the as-cast $(FeCoNi)_{95}Al_5$. Figure 1(b) exhibits the influence of Al contents on the lattice constants of MEAs based on the analysis of XRD results. It can be seen that the lattice constants increase linearly with the increase of Al contents. Figure 2 shows the microstructure of as-cast $(FeCoNi)_{71}Al_{23}$ MEA. The MEAs have non-uniformly distributed grains with a large size of ~460 μm.

Figure 3 shows the compressive strain−stress curves for as-cast $(FeCoNi)_{1-x}Al_x$ MEAs performed at room temperature. The MEA with Al content of 5 at.% has the lowest yield strength, which is about 89 MPa. When the content of Al increases from 5 to 9 at.%, the yield strength increases from 89 to 167 MPa. All the MEAs with low content of Al (x=5−9 at.%) exhibit the good

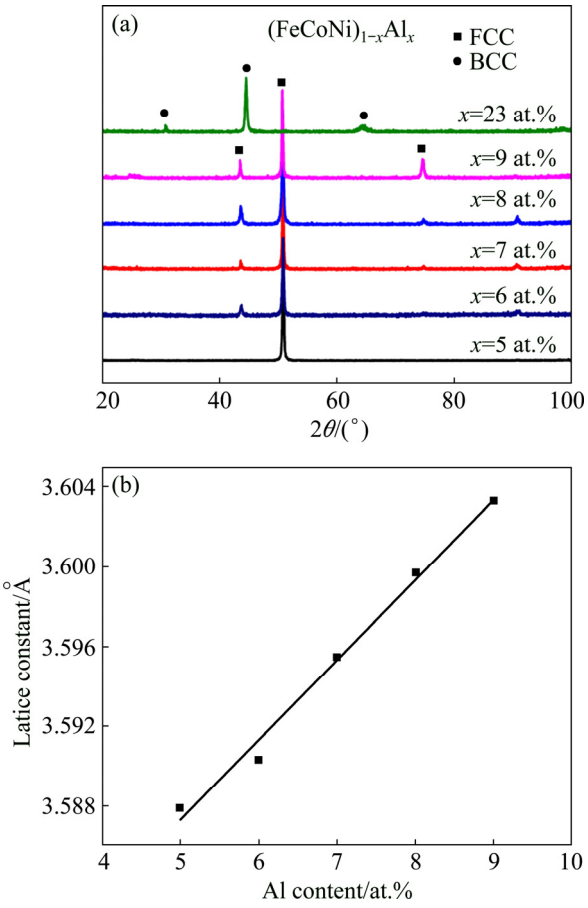

Fig. 1 XRD patterns (a) and lattice constants as function of Al contents (b) of $(FeCoNi)_{1-x}Al_x$ MEAs

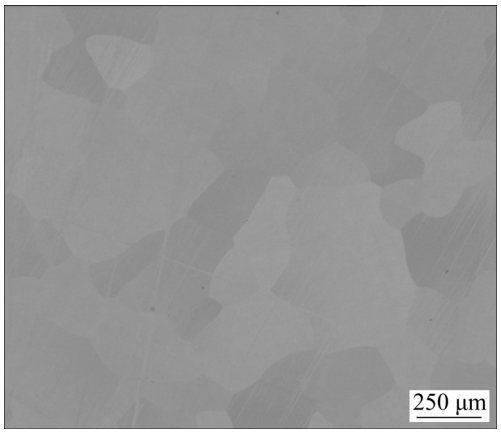

Fig. 2 Microstructure of $(FeCoNi)_{77}Al_{23}$ MEA

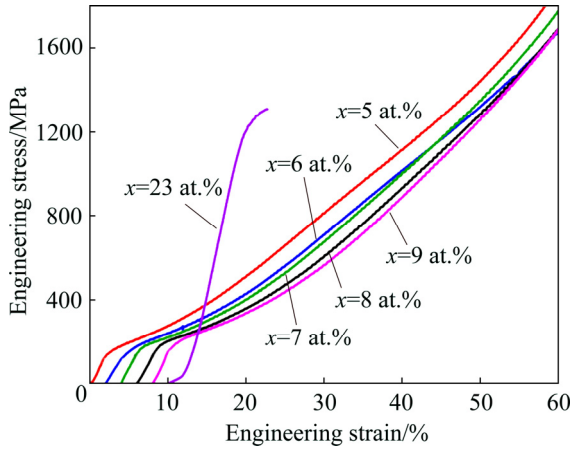

Fig. 3 Room-temperature compressive strain−stress curves for $(FeCoNi)_{1-x}Al_x$ MEAs

plasticity of over 60%. The MEA with the high content of Al (x=23 at.%) exhibits the highest yield strength (~1156 MPa) and the serious degradation of compressive plasticity (~10%).

Figure 4 presents microstructures of Sc-containing $(FeCoNi)_{94}Al_6$ MEAs examined by the SEM. With 0.06 at.% Sc, the $(FeCoNi)_{94}Al_6$ MEA has a single FCC phase (denoted as A in Fig. 4). When the content of Sc increases to 0.1 at.%, a new phase (B) forms along grain boundaries and phase B presents as a shape of dots or discontinuous strips. With the increase of Sc content, the area of phase B expands. The EDS analyses of Sc-containing $(FeCoNi)_{94}Al_6$ MEAs are shown in Table 1. It can be seen that FCC matrix phase mainly contains Fe, Co and Ni with nearly equimolar ratios. Phase B mainly consists of Ni and Sc. The molar ratio of Ni to Sc is about 2:1, which indicates that phase B may be the Ni_2Sc that is a kind of $MgCu_2$-type intermetallic [19]. The formation of intermetallic phases usually increases the strength of MEA with a single phase. Figure 5 shows the compressive strain−stress curves for Sc-containing $(FeCoNi)_{1-x}Al_x$ (x=5−9 at.%) MEAs at room temperature. The yield strengths of these MEAs are summarized in Fig. 6. All Sc-containing $(FeCoNi)_{1-x}Al_x$ (x=5−9 at.%) MEAs keep good plasticity, which is over 60%. A minor addition of Sc increases the yield strength of $(FeCoNi)_{1-x}Al_x$ MEAs significantly.

Figure 7 presents microstructures of $(FeCoNi)_{77}Al_{23}$ MEAs with different Sc contents. The $(FeCoNi)_{77}Al_{23}$ MEAs with different Sc contents exhibit the single BCC phase. When the content of Sc increases to 0.1 at.%, a new phase (C) begins to precipitate along grain boundaries. As the content of Sc reaches 0.3 at.%, phase C can also precipitate in the matrix, as shown in Figure 7(b). The average particle size of phase C is about 100 nm, and tens of precipitates usually get together in a special region. Due to the little size of precipitates, the

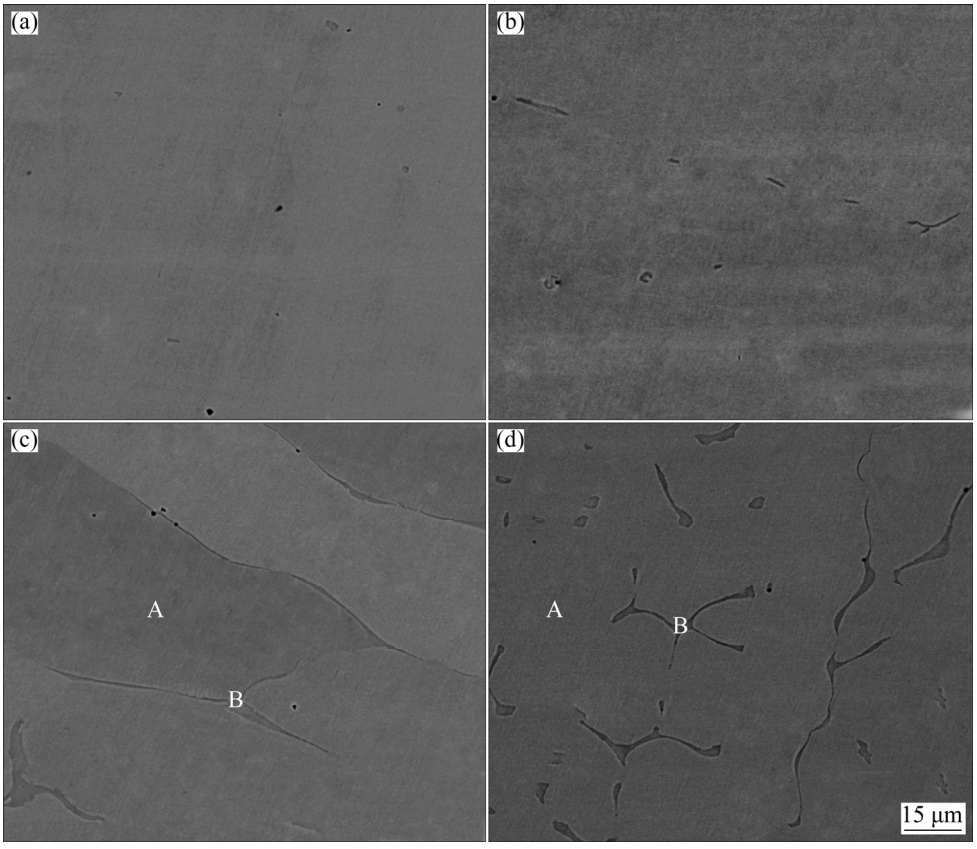

Fig. 4 Microstructures of Sc-containing $(FeCoNi)_{94}Al_6$ MEAs: (a) 0.06 at.% Sc; (b) 0.1 at.% Sc; (c) 0.3 at.% Sc; (d) 0.5 at.% Sc

Table 1 Chemical compositions of phases in Sc-containing $(FeCoNi)_{1-x}Al_x$ MEAs (at.%)

Phase	Fe	Co	Ni	Al	Sc
A	31.69	30.68	31.56	5.52	0.55
B	8.97	16.85	46.93	2.71	24.54

composition of phase C is hard to be analyzed by EDS in the SEM. However, based on the bright contrast in the backscatter electron images in Fig. 7, phase C may be AlSc phase [16]. Figure 8 shows compressive strain−stress curves of different Sc-containing $(FeCoNi)_{77}Al_{23}$ MEAs at room temperature. According to the compressive strain−stress curves, the addition of Sc has little effect on yield strength. As 0.1% and 0.3 at.% of Sc are added, the compressive plasticity of $(FeCoNi)_{77}Al_{23}$ MEA are enhanced from 8 % to 18%.

4 Discussion

4.1 Effect of Al on mechanical behavior of FeCoNi MEAs

As shown in Fig. 3, the addition of Al enhanced the yield strength of FeCoNi MEAs and the yield strength increased with the content of Al element. Strengthening mechanisms in $FeCoNiAl_x$ can be summarized into several aspects, including solid-solution hardening (σ_{ss}), grain-boundary hardening (σ_{gb}), precipitation hardening (σ_{ppt}) and dislocation hardening (σ_{dis}). In general, the

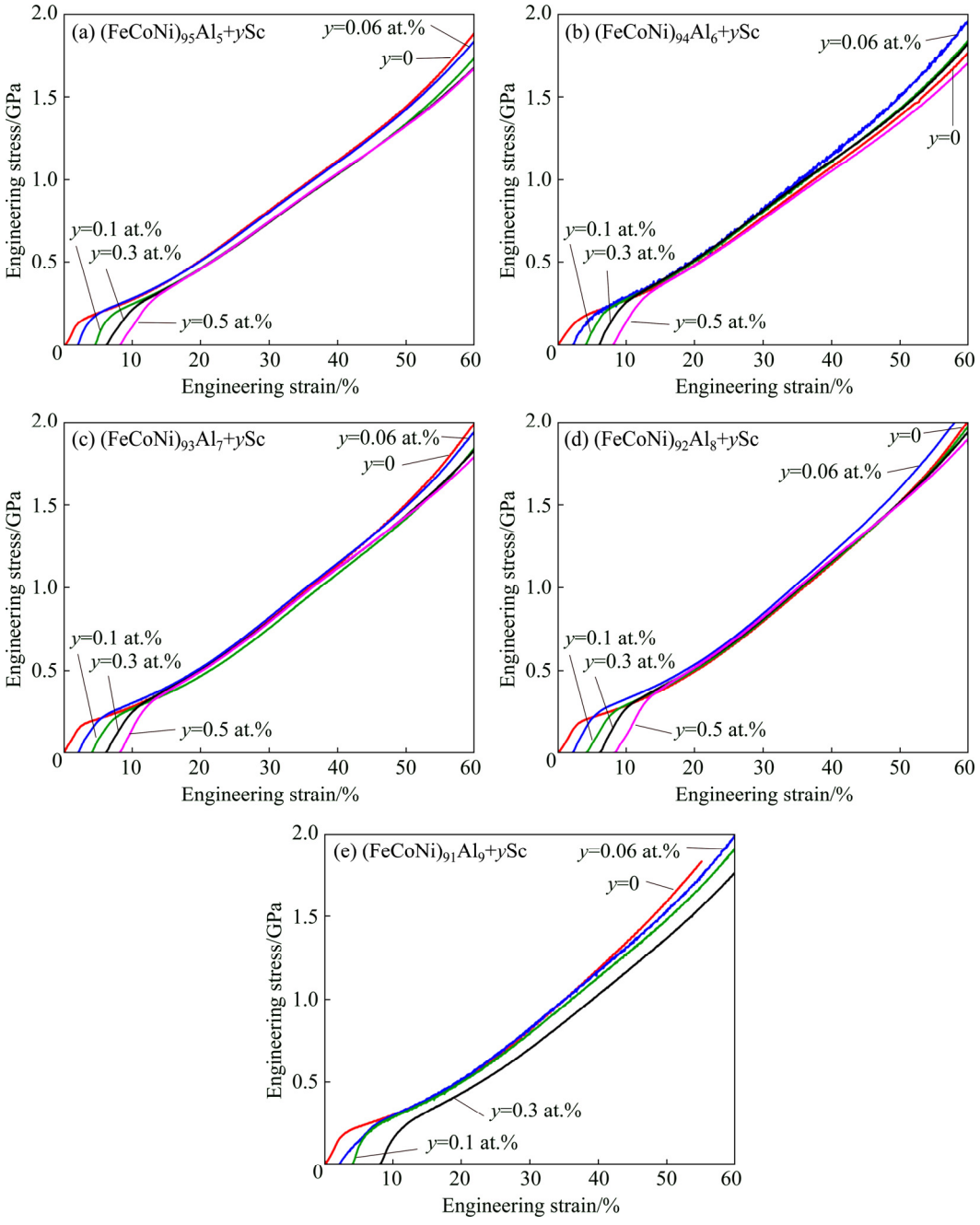

Fig. 5 Room-temperature compressive strain−stress curves for Sc-containing $(FeCoNi)_{1-x}Al_x$ (x=5−9 at.%) MEAs

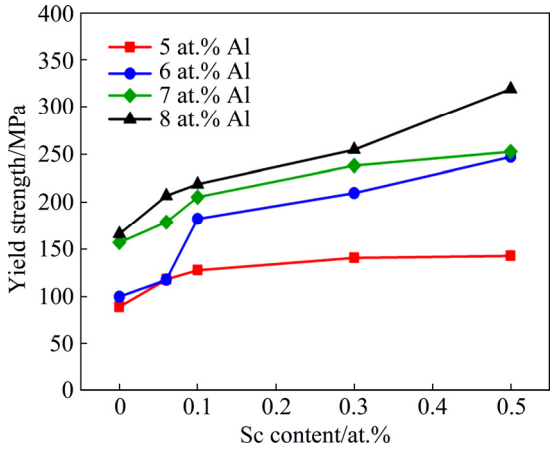

Fig. 6 Yield strength as function of Sc content in Sc-containing $(FeCoNi)_{1-x}Al_x$ MEAs

yield strength (σ_y) can be calculated by microstructure-related equation [14]:

$$\sigma_y=\sigma_A+\sigma_{ss}+\sigma_{ppt}+\sigma_{dis}+\sigma_{gb} \quad (1)$$

According to the microstructures measured by SEM and XRD, no precipitate formed in the matrix. As the $FeCoNiAl_x$ MEAs were prepared by arc-melting, the sizes of grain were around identical and there was almost no dislocation in the matrix. Therefore, the contributions of yield strength caused by precipitation strengthening, dislocation strengthening and grain boundary strengthening can be neglected.

In this work, σ_y can be calculated by the simplified equation:

$$\sigma_y=\sigma_A+\sigma_{ss} \quad (2)$$

where σ_A is the yield strength of the FeCoNi prepared by casting and the value of σ_A is 77 MPa [20]. The solid solution hardening is usually analyzed in dilute solution alloys. However, for MEA, it is hard to define the solute element and solvent element. Some researchers have attempted to predict the effect of solid solution hardening in MEAs [21,22]. A simple approach is treating the MEA with a single phase as a solvent matrix. In this work, FeCoNi MEA is treated as the matrix and Al element is considered as the solute. The analysis of substitutional solid solution strengthening is based on dislocation−solute elastic interactions. In $FeCoNiAl_x$ MEAs, Al plays a key role in solid solution strengthening and σ_{ss} can be calculated by equation as [14]

$$\sigma_{ss}=M\frac{G\varepsilon_s^{3/2}c^{1/2}}{700} \quad (3)$$

where M is the Taylor factor, which can convert shear strength to normal strength. The Taylor factor for a polycrystalline matrix is treated as 3.06. G is the shear modulus for the FeCoNi MEA, and c is the molar

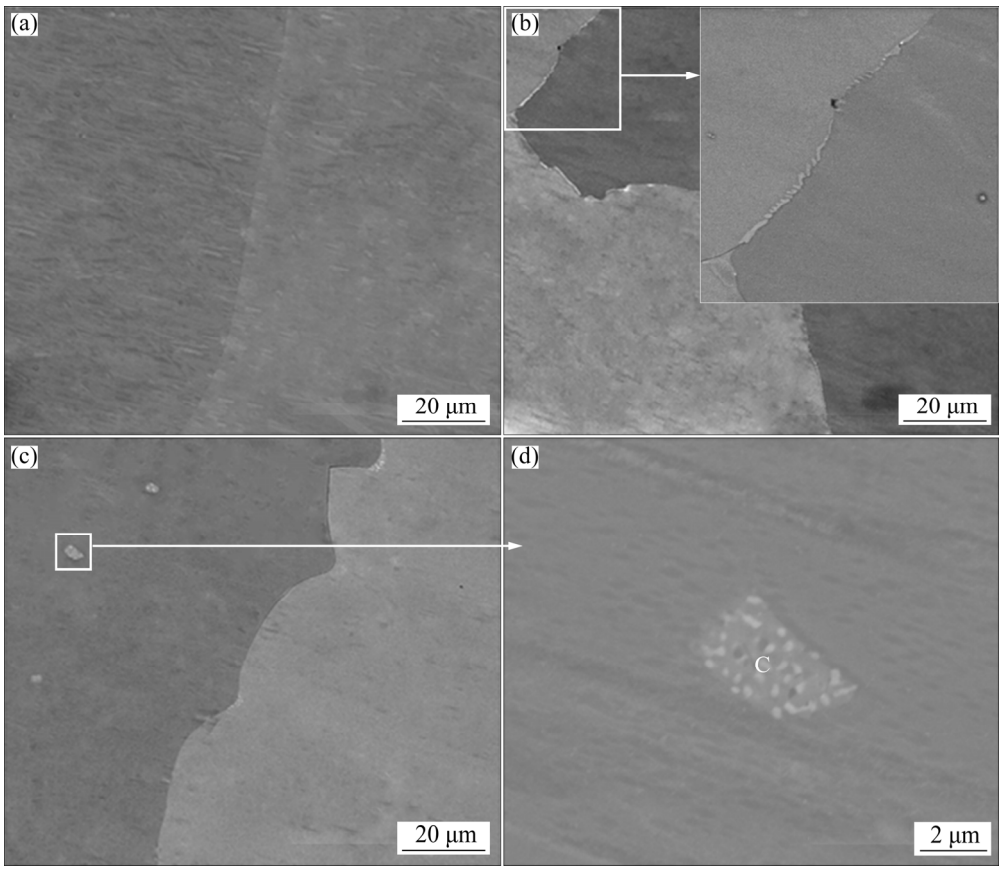

Fig. 7 Microstructures of Sc-containing $(FeCoNi)_{77}Al_{23}$ MEAs: (a) 0.06 at.% Sc; (b) 0.1 at.% Sc; (c, d) 0.3 at.% Sc

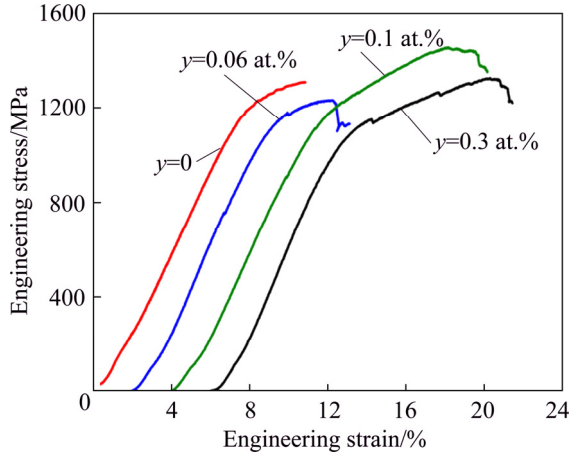

Fig. 8 Room-temperature compressive strain−stress curves for Sc-containing $(FeCoNi)_{77}Al_{23}$ MEAs

fraction of Al element. ε_s is the interaction parameter and it can be calculated by equations:

$$\varepsilon_s = \left| \frac{\varepsilon_G}{1+0.5\varepsilon_G} - 3\varepsilon_a \right| \quad (4)$$

$$\varepsilon_G = \frac{1}{G}\frac{\partial G}{\partial c} \quad (5)$$

$$\varepsilon_a = \frac{1}{a}\frac{\partial a}{\partial c} \quad (6)$$

where ε_G and ε_a represent the effects caused by elastic and atomic size mismatches, respectively. a is the lattice constant for the FeCoNi MEA.

The ε_a can be calculated from the lattice parameters, as shown in Table 2. Compared with parameter of ε_a, the value of ε_G is small and can be neglected. The solid solution hardening (σ_{ss}) is calculated and the results are given in Table 2. Figure 9 shows the comparison between the predicted (σ_{Pre}) and experimental yield strength (σ_{Exp}). It can be seen that the increments of yield strength of $FeCoNiAl_x$ MEAs are largely attributed to solid solution strengthening. With the increase of Al content from 5 to 9 at.%, the predicted and experimental yield strength increase almost linearly [23]. The slope of σ_{Pre} is slightly higher than that of σ_{Exp}. This may be caused by other strengthening mechanism.

According to solid solution hardening mechanism, the σ_{Pre} of $FeCoNiAl_{23}$ is about 525 MPa. But the σ_{Exp} of $FeCoNiAl_{23}$ is about 1150 MPa, which is significantly larger than σ_{Pre}. Therefore, for $FeCoNiAl_x$ with high content of Al, solid solution hardening is not the dominant hardening mechanism. In $FeCoCrNiMnAl_x$ MEA, when the content of Al is in the range of 8−16 at.%, the phase transformation occurred and BCC phases began to form in FCC matrix. The yield strength increases drastically and a good linear relationship is observed between increment of yield strength and volume fraction of BCC phase. The increment in yield strength per volume percent of BCC is 27.3 MPa [24]. That means that, for $FeCoNiAl_x$ with high content of Al, the formation of BCC plays the dominant role in the improvement of yield strength.

Table 2 Composition of Al (c), lattice constants (a), solid-solution hardening (σ_{ss}) and predicted yield strength (σ_p) for $FeCoNiAl_x$ MEAs

Alloy	c/at.%	a/Å	σ_{ss}/MPa	σ_p/MPa
$FeCoNiAl_{0.05}$	5	3.5879	20.8	97.8
$FeCoNiAl_{0.06}$	6	3.5903	27.5	104.5
$FeCoNiAl_{0.07}$	7	3.5955	41.9	118.9
$FeCoNiAl_{0.08}$	8	3.5997	56.3	133.3
$FeCoNiAl_{0.09}$	9	3.6033	70.9	147.9

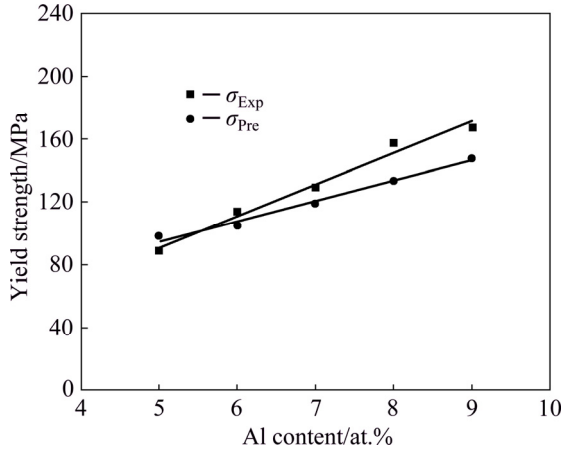

Fig. 9 Experimental and predicted yield strength of $FeCoNiAl_x$ MEAs

4.2 Effect of Sc on mechanical behavior of FeCoNiAl MEA

For the Sc-containing $(FeCoNi)_{1-x}Al_x$ (x=5−9 at.%) MEAs, the increment of yield strength is caused by solid solution hardening (σ_{ss}) and secondary phase hardening (σ_{sp}). When the content of Sc is 0.06 at.%, Sc-containing $(FeCoNi)_{1-x}Al_x$ MEAs keep a single FCC phase. Solid solution hardening plays the dominant role in the increment of yield strength. As the content of Sc increases to 0.1 at%, $MgCu_2$-type intermetallic phase forms. With fewer available slip systems, intermetallic phase is more brittle but stronger than FCC matrix. Therefore, the volume fraction and strength of Ni_2Sc have a significant effect on the yield strength of Sc-containing $(FeCoNi)_{1-x}Al_x$ MEAs. As the strength of the duplex alloy is generally described by the simple rule-of-mixture, the yield strength of Sc-containing $(FeCoNi)_{1-x}Al_x$ MEAs can be calculated by [24]

$$\sigma_y = \sigma_{fcc}V_{fcc} + \sigma_{sp}V_{sp} \quad (7)$$

where σ_{fcc} and σ_{sp} are the yield strengths of the FCC phase and secondary intermetallic phase, respectively.

V_{fcc} and V_{sp} are the volume fractions of the FCC phase and secondary intermetallic phase, respectively. Consequently, with the increase in the content of Sc, the volume fraction of secondary intermetallic phase increases and the volume fraction of FCC phase decreases. Since the yield strength of secondary intermetallic phase is larger than that of FCC phase, the yield strength increases.

For the Sc-containing $(FeCoNi)_{77}Al_{23}$ MEAs, the addition of Sc has little effect on yield strength. In fact, with the high content of Al (23 at.%), the solid solution hardening of $(FeCoNi)_{77}Al_{23}$ MEA has reached a high level. According to Eq. (7), the volume fraction of AlSc phase is too small and the increment of yield strength contributed by secondary phase hardening can be neglected. Furthermore, the formation of AlSc phase in special region may lead to the stress−strain concentrations. As the size of AlSc is as fine as around 100 nm, it makes the fracture hard to occur. The AlSc phase may help to impede the propagation of micro-cracks and the compressive plasticity is improved.

5 Conclusions

(1) $(FeCoNi)_{1-x}Al_x$ (x=5−9 at.%) MEAs have a single FCC crystal structure. The lattice constants increase linearly with the increase of Al content.

(2) In $(FeCoNi)_{1-x}Al_x$ (x=5−9 at.%) MEAs, the predicted values and experimental values of the yield strength increase almost linearly with the increase of Al content. The increment of yield strength of $FeCoNiAl_x$ MEAs is largely contributed by solid solution hardening.

(3) In Sc-containing $(FeCoNi)_{1-x}Al_x$ (x=5−9 at.%) MEAs, Ni_2Sc intermetallic phase can form at the grain boundaries. In Sc-containing $(FeCoNi)_{77}Al_{23}$ MEAs, the precipitates can form at grain boundaries and in the matrix.

(4) In Sc-containing $(FeCoNi)_{1-x}Al_x$ (x=5−9 at.%) MEAs, a minor addition of Sc can significantly increase the yield strength. In Sc-containing $(FeCoNi)_{77}Al_{23}$ MEAs, the addition of Sc has little effect on yield strength but can improve the compressive plasticity.

References

[1] ZHANG Yong, ZUO Ting-ting, TANG Zhi, GAO M, DAHMEN K, LIAW P K. Microstructures and properties of high-entropy alloys [J]. Progress in Materials Science, 2014, 61: 1−93.

[2] CANTOR B, CHANG I T H, KNIGHT P, VINCENT A J B. Microstructural development in equiatomic multicomponent alloys [J]. Materials Science and Engineering A, 2004, 375(Supplement C): 213−218.

[3] WANG Zhi-peng, FANG Qi-hong, LI Jia, LIU Bin, LIU Yong. Effect of lattice distortion on solid solution strengthening of BCC high-entropy alloys [J]. Journal of Materials Science and Technology, 2018, 34(2): 349−354.

[4] ZHOU Rui, CHEN Gang, LIU Bin, WANG Jia-wen, HAN Liu-liu, LIU Yong. Microstructures and wear behaviour of $(FeCoCrNi)_{1-x}(WC)_x$ high entropy alloy composites [J]. International Journal of Refractory Metals and Hard Materials, 2018, 75: 56−62.

[5] KUKSHAL V, PATNAIK A, BHAT I K. Corrosion and thermal behaviour of $AlCr_{1.5}CuFeNi_2Ti_x$ high-entropy alloys [J]. Materials Today: Proceedings, 2018, 5(9, Part 1): 17073−17079.

[6] LI Bao-yu, PENG Kun, HU Ai-ping, ZHOU Ling-ping, ZHU Jia-jun, LI De-yi. Structure and properties of $FeCoNiCrCu_{0.5}Al_x$ high-entropy alloy [J]. Transactions of Nonferrous Metals Society of China, 2013, 23(3): 735−741.

[7] LIU Yi-xuan, CHENG Cong-qian, SHANG Jian-lu, WANG Rui, LI Peng, ZHAO Jie. Oxidation behavior of high-entropy alloys AlxCoCrFeNi (x=0.15, 0.4) in supercritical water and comparison with HR3C steel [J]. Transactions of Nonferrous Metals Society of China, 2015, 25(4): 1341−1351.

[8] CHEN Qiu-shi, LU Yi-ping, DONG Yong, WANG Tong-min, LI Ting-ju. Effect of minor B addition on microstructure and properties of AlCoCrFeNi multi-component alloy [J]. Transactions of Nonferrous Metals Society of China, 2015, 25(9): 2958−2964.

[9] WU Z, BEI H, PHARR G M, GEORGE E P. Temperature dependence of the mechanical properties of equiatomic solid solution alloys with face-centered cubic crystal structures[J]. Acta Materialia, 2014, 81: 428−441.

[10] ZHOU Rui, LI Mou, WU Hong, LIU Bin, LIU Yong. Effect of multi-component carbides on the mechanical behavior of a multi-element alloy [J]. Materials Science and Engineering A, 2019, 758: 99−102.

[11] WANG Woei-ren, WANG Wei-lin, WANG Shang-chih, TSAI Y C, LAI C H, YEH J W. Effects of Al addition on the microstructure and mechanical property of AlxCoCrFeNi high-entropy alloys [J]. Intermetallics, 2012, 26: 44−51.

[12] ZUO T T, LI R B, REN X J, ZHANG Y. Effects of Al and Si addition on the structure and properties of CoFeNi equal atomic ratio alloy [J]. Journal of Magnetism and Magnetic Materials, 2014, 371: 60−68.

[13] LIU Y Y, CHEN Z, SHI J C, WANG Z Y, ZHANG J Y. The effect of Al content on microstructures and comprehensive properties in Al_xCoCrCuFeNi high entropy alloys [J]. Vacuum, 2019, 161: 143−149.

[14] HE J Y, WANG H, HUANG H L, XU X D, CHEN M W, WU Y, LIU X J, NIEH T G, AN K, LU Z P. A precipitation-hardened high-entropy alloy with outstanding tensile properties [J]. Acta Materialia, 2016, 102: 187−196.

[15] YANG T, ZHAO Y L, TONG Y, JIAO Z B, WEI J, CAI J X, HAN X D, CHEN D, HU A, KAI J J, LU K, LIU Y, LIU C T. Multicomponent intermetallic nanoparticles and superb mechanical behaviors of complex alloys [J]. Science, 2018, 362(6417): 933−937.

[16] YUSENKO K V, RIVA S, CRICHTON W A, SPEKTOR K, BYKOVA E, PAKHOMOVA A, TUDBALL A, KUPENKO I, ROHRBACH A, KIEMME S, MAZZALI F, MARGADONNA S, LAVER Y N, BROWN S. High-pressure high- temperature tailoring of high entropy alloys for extreme environments [J]. Journal of Alloys and Compounds, 2018, 738: 491−500.

[17] XU Pian, JIANG Feng, TANG Zhong-qin, YAN Ning, JIANG Jing-xu, XU Xu-da, PENG Yong-yi. Coarsening of Al_3Sc precipitates in Al−Mg−Sc alloys [J]. Journal of Alloys and Compounds, 2019, 781: 209−215.

[18] TAENDL J, ORTHACKER A, AMENITSCH H, KOTHLEITNER G, POLETTI C. Influence of the degree of scandium supersaturation on the precipitation kinetics of rapidly solidified Al−Mg−Sc−Zr alloys [J]. Acta Materialia, 2016, 117: 43−50.

[19] FAN L, HE J Q, LIU H S, PENG H L, JIN Z P. Measurement of phase equilibria in Zr−Ni−Sc ternary system [J]. Calphad, 2019, 65: 25−33.

[20] VARVENNE C, LUQUE A, CURTIN W A. Theory of strengthening in fcc high entropy alloys [J]. Acta Materialia, 2016, 118: 164−176.
[21] TODA-CARABALLO I, WRÓBEL J S, DUDAREV S L, NGUYEN- MANH D, RIVERA-DÍAZ-DEL-CASTILLO P E J. Interatomic spacing distribution in multicomponent alloys [J]. Acta Materialia, 2015, 97: 156−169.
[22] MOON J, JANG M J, BAE J W, YIM D, PARK J M, LEE J, KIM H S. Mechanical behavior and solid solution strengthening model for face-centered cubic single crystalline and polycrystalline high-entropy alloys [J]. Intermetallics, 2018, 98: 89−94.
[23] AGUSTIANINGRUM M P, YOSHIDA S, TSUJI N, PARK N. Effect of aluminum addition on solid solution strengthening in CoCrNi medium-entropy alloy [J]. Journal of Alloys and Compounds, 2019, 781: 866−872.
[24] HE J Y, LIU W H, WANG H, WU Y, LIU X J, NIEH T G, LU Z P. Effects of Al addition on structural evolution and tensile properties of the FeCoNiCrMn high-entropy alloy system [J]. Acta Materialia, 2014, 62: 105−113.

Al 和 Sc 元素对 FeCoNi 多组元合金变形行为的影响

周 睿[1]，李 谋[1]，邱敬文[1,2]，欧阳思慧[1]，潘 迪[1]，周承商[1]，刘 咏[1]

1. 中南大学 粉末冶金国家重点实验室，长沙 410083；
2. 湖南科技大学 难加工材料高效精密加工湖南省重点实验室，湘潭 411201

摘 要：研究 Al 和 Sc 元素的添加对 FeCoNi 多组元合金显微组织与力学性能的影响，并讨论强化机制。结果表明，在 FeCoNi 多组元合金中添加少量的 Al 元素，合金仍能保持 FCC 单相结构；随着 Al 元素含量的增加，多组元合金的屈服强度呈线性提高，其强化机制以固溶强化为主。另外，在$(FeCoNi)_{1-x}Al_x$多组元合金中引入 Sc 元素能够诱导合金内形成新相；添加微量的 Sc 元素能够有效提高低 Al 含量$(FeCoNi)_{1-x}Al_x$多组元合金的屈服强度，并能改善高 Al 含量$(FeCoNi)_{1-x}Al_x$多组元合金的压缩塑性。

关键词：FeCoNi 多组元合金；力学性能；显微组织；强化机制

(Edited by Bing YANG)